JOURNAL OF MATERIALS SCIENCE 32 (1997) 1925–1929

Study on the structures of N-containing melilite $Y_2Si_3O_3N_4$ and $Nd_2Si_{2.5}Al_{0.5}O_{3.5}N_{3.5}$

P. L. WANG
State Key Lab of High Performance Ceramics and Superfine Microstructure, Shanghai Institute of Ceramics, Chinese Academy of Sciences, Shanghai 200050, Peoples Republic of China

P.-E. WERNER
Department of Structural Chemistry, Arrhenius Lab, University of Stockholm, S-10691 Stockholm, Sweden

Rietveld refinements have been used to determine the structure of $Y_2Si_3O_3N_4$ from X-ray data and $Nd_2Si_{2.5}Al_{0.5}O_{3.5}N_{3.5}$ from neutron powder diffraction data. The refinements show that in the melilite phase $Y_2Si_3O_3N_4$ and melilite solid solution $Nd_2Si_{2.5}Al_{0.5}O_{3.5}N_{3.5}$ the distributions of cations and anions are almost identical. They are analogous to the akermanite ($Ca_2MgSi_2O_7$) structure, with Si/Si,Al atoms at the origin and centre of the unit cell and with four N/N,O atoms forming the SiN_4/(Si,Al)($N_{3.5}O_{0.5}$) tetrahedra which share corners with SiO_2N_2/(Si,Al)$O_{2.25}N_{1.75}$ tetrahedra to form a continuous sheet structure. Each Y^{3+} or Nd^{3+} ion is surrounded by eight N/O atoms forming the coordination polyhedron in $Y_2Si_3O_3N_4$ and $Nd_2Si_{2.5}Al_{0.5}O_{3.5}N_{3.5}$ respectively. The arrangement of Al, Si atoms in the tetrahedra in $Nd_2Si_{2.5}Al_{0.5}O_{3.5}N_{3.5}$ structure is also discussed.

1. Introduction

Nitrogen-containing melilite phases (abbreviated as M) comprise compounds based on the general melilite composition $Si_3N_4 \cdot R_2O_3$ with R = Y and rare earth elements such as Nd, Sm, Gd and Dy. Recent work [1–4] indicates that aluminium can be dissolved in melilite, forming $R_2Si_{3-x}Al_xO_{3+x}N_{4-x}$ solid solutions. Our previous results [4] indicate that the solubility of Al in melilite solid solutions (abbreviated as M′) decreases with decreasing ionic radius of the rare earth element. Up to one Si can be replaced by Al in the Nd–M′ phase, whereas yttrium melilite has the lowest observed aluminium solubility of about $x = 0.6$.

Yttria and rare earth oxides are frequently used as sintering aids in the preparation of α-Sialon ($R_xSi_{12-(m+n)}Al_{m+n}O_nN_{16-n}$) ceramics. Consequently nitrogen-containing melilite phases and solid solutions are frequently observed as grain boundary phases in α-Sialon and mixed α-β-Sialon ceramics [5, 6]. R–M/R–M′ are the only stable intergranular phases with high nitrogen contents in the R–Si–Al–O–N (R = Nd,Sm) systems [7] and thus are an important intergranular phase in α-Sialon or mixed α-β-Sialon ceramics. However, the poor oxidation resistance of Y–M ($Y_2Si_3O_3N_4$) at high temperatures [8] has given the R–M phase a bad reputation as an intergranular phase in Sialon materials, whereas the R–M′ phases are expected to have an improved stability against oxygen, because some of the Si–N is replaced by Al–O. Since the high temperature properties of Sialon ceramics are mainly determined by deterioration of the grain boundary phase, studies on the R–M/R–M′ phases to elucidate information on their formation, solubility limits and behaviour at high temperatures have attracted considerable attention [3, 4, 9].

Melilite is analogous to akermanite ($Ca_2MgSi_2O_7$), [10] in which [MgO_4] tetrahedra are located at the origin and centre of the unit cell and are linked with [Si_2O_7] groups. Each Ca^{2+} ion is surrounded by eight O atoms forming a polyhedron (Fig. 1). The sheets of tetrahedra are linked parallel to the (0 0 1) direction. The single crystal structure of $Ca_2MgSi_2O_7$ was determined more than forty years ago. It is now possible to investigate structures from polycrystalline diffraction data using the whole-pattern fitting technique of Rietveld [11]. In order to understand the solubility limits of Al in R–M′ phases it would be of interest to know the distribution of Si(Al), O and N atoms in R–M/R–M′. The determination of accurate coordinates may also provide a firm basis for the application of crystal-chemistry arguments to the possible substitutions in the melilite structure.

2. Experimental procedure

Samples of the Y–M phase $Y_2Si_3O_3N_4$ and Nd–M′ phase $Nd_2Si_{3-x}Al_xO_{3+x}N_{4-x}$ ($x = 0.5$) were prepared by the hot-pressing technique (20 MPa) in flowing N_2 at 1750 °C and 1675 °C for 1 h, respectively [4]. The synthesized samples were identified by X-ray

0022–2461

diffraction (XRD) and it was found that the major phase was melilite with a very small amount of the J phase $R_4Si_2O_7N_2$ (R = Y, Nd) also being present. The unit cells of these two phases were refined, using Si powder as an internal standard, from X-ray Guinier–Hägg camera diffraction patterns (Cu$K\alpha_1$ radiation, $\lambda = 0.15405981$ nm) evaluated with a computer-controlled film scanner and associated programs [12, 13] (see Table I). X-ray powder diffraction data for $Y_2Si_3O_3N_4$ were collected at 295 K with a Stoe STADI/P diffractometer in transmission mode. A germanium monochromator with a 220 mm radius of curvature was used to obtain strictly monochromatic Cu$K\alpha_1$ radiation. The data collections were performed with a small linear position sensitive detector, covering 4° in 2θ with a resolution of 0.01°(2θ). In order to reduce the influence of errors in the intensity calibration of the detector, it was moved in steps of 0.2°, thus giving an average intensity from 20(= 4.0/0.2) measurements at each theta position. Data was collected between 15–95° (2θ) in steps of 0.02°, with a measuring time of 220 s per step. This data was then used in the subsequent structure refinements. For $Nd_2Si_{2.5}Al_{0.5}O_{3.5}N_{3.5}$ neutron powder diffraction data ($\lambda = 0.1470$ nm) was used in the structure refinement. The data collections were performed at the Swedish Studsvik R2 reactor and data was obtained in a range of 2θ of 10–109.4° in steps of 0.08°, with a measuring time of 3 min per step.

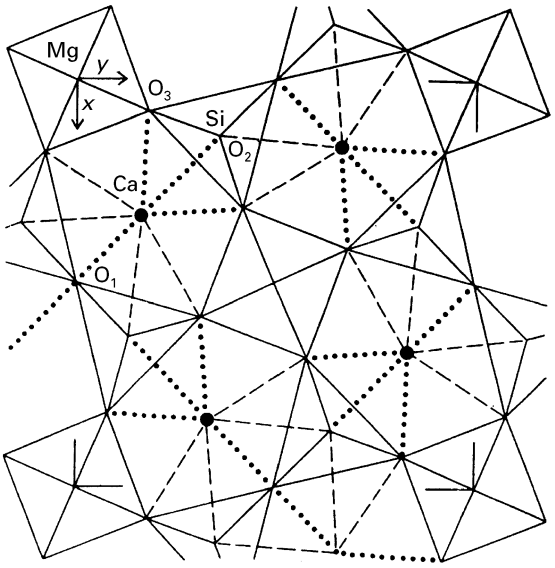

Figure 1 Projection of the akermanite ($Ca_2MgSi_2O_7$) structure along to the (0 0 1) direction [10]. The tetrahedra are outlined by solid lines. The dashed lines show long Ca–O distances and the heavy dotted lines show short Ca–O distances.

TABLE I Summary of unit cell and refinement details

	$Y_2Si_3O_3N_4$	$Nd_2Si_{2.5}Al_{0.5}O_{3.5}N_{3.5}$
Space group	$P\bar{4}2_1m$	$P\bar{4}2_1m$
a(nm)	0.76137(2)	0.77462(5)
c(nm)	0.49147(2)	−0.50390(4)
Radiation	CuK_{α_1}	neutrons
Wavelength (nm)	0.15405981	0.1470
2θ scan range (°)	15–95	10–109.4
Number of structural parameters	17	12/13
Number of profile parameters	11	11
Number of unique reflections	100	152
R_F*	0.053	0.077
R_B	0.066	0.128
R_P	0.068	0.075
R_{WP}	0.085	0.097
V	−0.014(1)	−1.19(7)
W	0.024(1)	0.30(2)

*Reliability index R can be defined as R_F, R_B, R_P, R_{WP}, R_F: R value for structure amplitudes, R_B: R value for Bragg intensities, R_P: the pattern R factor, R_{WP}: the weighted pattern R factor.

3. Structure refinement

The Rietveld refinements were performed with a version of the refinement program written by Wiles *et al.* [14]. The atomic parameters of $Ca_2MgSi_2O_7$ [10] were used as the starting parameters and the position of the N atom was chosen to be located (in Wyckoff notation) at the 8/f position of space group $P\bar{4}2_1m$. The background intensity Y_{bi} at the ith step was described by the polynomial

$$Y_{bi} = \sum_{m=0}^{5} B_m[(2\theta_i/\mathrm{BKPOS}) - 1]^m \qquad (1)$$

where B_m are parameters to be refined and BKPOS is origin of polynomial for background, 30 degrees (2θ) used in this work. The peak shape used was a Pearson VII function for the X-ray and a Gaussian function for the neutron data. The extent of a peak was taken to be 3.0 times the FWHM (full-width at half-maximum), H_k, on either side of the peak centre. H_k was given by $H_k = U\tan^2\theta_k + V\tan\theta_k + W$, where U, V, W are the width parameters and k is the reflection index. The final refinements of $Y_2Si_3O_3N_4$ involved one scale factor, the zero-point position, two peak half-width parameters (V, W), the unit cell dimensions, peak shape parameters, an absorption correction factor, background and crystal-structure parameters, i.e., ten atom coordinates and four isotropic temperature factors. Some refinement details are shown in Table 1. In order to locate the Al positions in the structure of $Nd_2Si_{2.5}Al_{0.5}O_{3.5}N_{3.5}$, two kinds of possible substitutions of Al for Si have been tried in the refinements, i.e., one Al atom distributed in either position 4/e or 2a respectively. The initial atom coordinates used to refine the neutron data of $Nd_2Si_{2.5}Al_{0.5}O_{3.5}N_{3.5}$ were the final parameters obtained from the X-ray refinement. No absorption or peak shape corrections were made, and a common isotropic temperature factor was used for all the atoms. The refinement was terminated when all shifts in the parameters were less than 10% of the corresponding standard deviations. The final R values and some essential data are listed in Table 1, and final atomic coordinates in Table II. The relative large standard deviations for Si in $Nd_2Si_{2.5}Al_{0.5}O_{3.5}N_{3.5}$ and N in $Y_2Si_3O_3N_4$ are due to the low neutron and X-ray scattering amplitudes of Si and N atoms.

TABLE II Final atomic positional coordinates and isotropic temperature factors for $Y_2Si_3O_3N_4$ and $Nd_2Si_{2.5}Al_{0.5}O_{3.5}N_{3.5}$

Atom	Wyckoff notation	Coordinates	$Y_2Si_3O_3N_4$	$Nd_2Si_{2.5}Al_{0.5}O_{3.5}N_{3.5}$ (model 1)
M (Y/Nd)	4/e	x	0.3363(1)	0.3347(6)
		y	0.1637(1)	0.1653(6)
		z	0.5028(4)	0.4945(13)
		$B(\times 10^{-2}\,nm^2)$	1.0(2)	0.13(6)
Si1 ($Si/Si_{0.75}Al_{0.25}$)	4/e	x	0.1442(4)	0.1453(12)
		y	0.3558(4)	0.3547(12)
		z	0.9407(10)	0.9440(22)
		$B(\times 10^{-2}\,nm^2)$	0.8(2)	0.13(6)
Si2	2/a	x	0.0	0.0
		y	0.0	0.0
		z	0.0	0.0
		$B(\times 10^{-2}\,nm^2)$	0.8(2)	0.13(6)
O1	2/c	x	0.5	0.5
		y	0.0	0.0
		z	0.1942(29)	0.1773(26)
		$B(\times 10^{-2}\,nm^2)$	1.0(3)	0.13(6)
O2	4/e	x	0.1435(11)	0.1384(7)
		y	0.3565(11)	0.3616(7)
		z	0.2827(17)	0.2855(16)
		$B(\times 10^{-2}\,nm^2)$	1.0(3)	0.13(6)
N ($N/N_{0.875}O_{0.125}$)	8/f	x	0.0926(11)	0.0821(4)
		y	0.1623(11)	0.1644(5)
		z	0.7948(17)	0.8068(9)
		$B(\times 10^{-2}\,nm^2)$	0.1(3)	0.13(6)

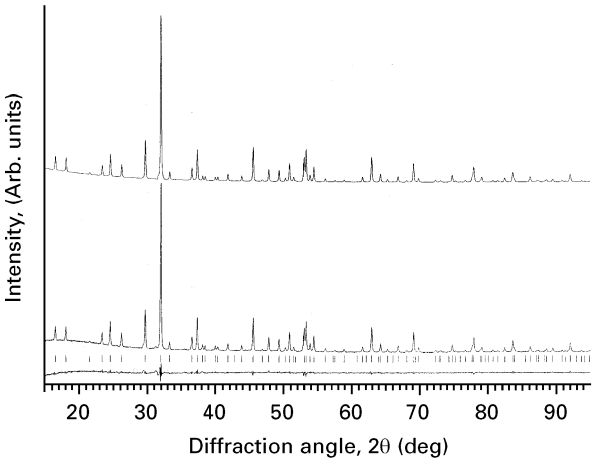

Figure 2 Output from a Rietveld analysis of the diffraction pattern from $Y_2Si_3O_4N_3$. The upper pattern is the calculated profile and the middle pattern is the observed X-ray data. The short vertical lines below the patterns represent the positions of all possible Bragg reflections for $Y_2Si_3O_4N_3$. The lower trace is the difference between the calculated and observed intensity at each step, plotted on the scale.

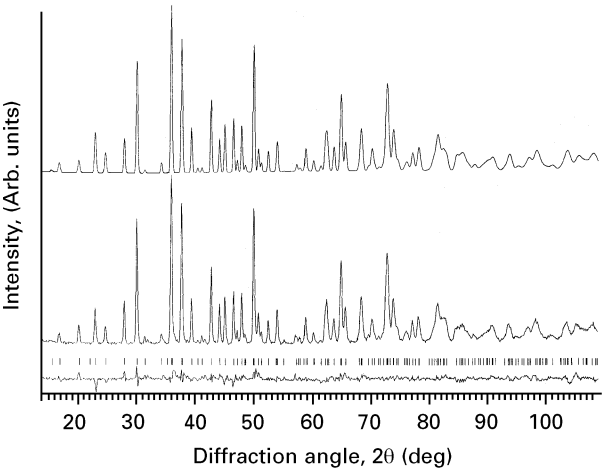

Figure 3 Output from a Rietveld analysis of the diffraction pattern from $Nd_2Si_{2.5}Al_{0.5}O_{3.5}N_{3.5}$. The upper pattern is the calculated profile and the middle pattern is the observed neutron data. The short vertical lines below the patterns represent the positions of all possible Bragg reflections for $Nd_2Si_{2.5}Al_{0.5}O_{3.5}N_3$. The lower trace is the difference between the calculated and observed intensity at each step, plotted on the scale.

The fit between the observed and calculated patterns for $Y_2Si_3O_3N_4$ and $Nd_2Si_{2.5}Al_{0.5}O_{3.5}N_{3.5}$ are shown in Figs 2 and 3.

4. Discussion

Some selected interatomic distances for $Y_2Si_3O_3N_4$ and $Nd_2Si_{2.5}Al_{0.5}O_{3.5}N_{3.5}$ are summarized in Table III. Projections of the $Y_2Si_3O_3N_4$ structure along the (1 0 0) and (0 0 1) directions are shown in Fig. 4(a and b). Comparing the $Y_2Si_3O_3N_4$ structure with akermanite $Ca_2MgSi_2O_7$, it can be observed that the Y atom and one Si atom in the $Y_2Si_3O_3N_4$ structure occupy the same positions as do Ca and Mg in $Ca_2MgSi_2O_7$, while N is located at the 8/f site of space group $P\bar{4}2_1m$ (No. 113). In the structure of $Nd_2Si_{2.5}Al_{0.5}O_{3.5}N_{3.5}$, the distributions of cations and anions are almost the same as in $Y_2Si_3O_3N_4$, except for the partial substitutions of Al and O for Si and N atoms. The arrangement of Al and Si atoms in $Nd_2Si_{2.5}Al_{0.5}O_{3.5}N_{3.5}$ is of interest, since they may be distributed in a number of ways inside the tetrahedra because of their similar ionic radii. The two extreme cases of ordering are, (a) 1 Si in position 2/a and 0.25 Al and 0.75 Si in position 4/e (model 1), (b) 0.5 Si and

TABLE III Some selected interatomic distances (nm) in $Y_2Si_3O_3N_4$and $Nd_2Si_{2.5}Al_{0.5}O_{3.5}N_{3.5}$ (units see Table I)

	$Y_2Si_3O_3N_4$	$Nd_2Si_{2.5}Al_{0.5}O_{3.5}N_{3.5}$
M (Y/Nd)–O1	0.2325(9)	0.2416(10)
–O2	0.2341(8)	0.2394(8)
–N(×2)	0.2346(8)	0.2511(7)
–O2(×2)	0.2570(8)	0.2609(8)
–N(×2)	0.2775(8)	0.2778(6)
Average	0.2506(8)	0.2576(8)
(Si/Si,Al) 1–O2	0.1681(10)	0.1724(14)
–N(×2)*	0.1685(9)	0.1700(10)
–O1	0.1688(7)	0.1705(11)
Average	0.1685(9)	0.1707(11)
(Si/Si,Al) 2–N(×4)**	0.1744(8)	0.1725(4)

*It should be $N_{1.75}O_{0.25}$ in $Nd_2Si_{0.25}Al_{0.5}O_{3.5}N_{3.5}$
**It should be $N_{3.5}O_{0.5}$ in $Nd_2Si_{2.5}Al_{0.5}O_{3.5}N_{3.5}$

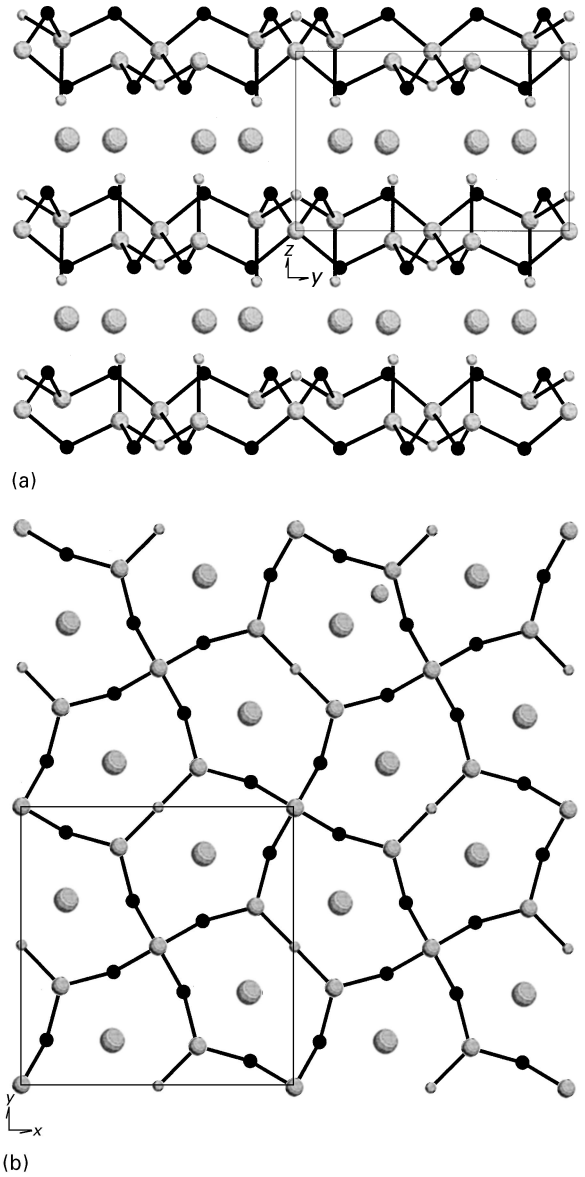

Figure 4 Projections of the $Y_2Si_3O_4N_3$ structure along (a) the (1 0 0) direction and (b) the (0 0 1) direction. The shaded circles, in the decreasing order of size, represent Y, Si and O atoms, and the filled circle represents N.

0.5 Al in position 2/a and 1 Si in position 4/e (model 2), in which the Al and Si atoms would be statistically distributed in the tetrahedra. However, the results of refinements indicated that there was no obvious difference between the two models. High resolution neutron data is in practice necessary to distinguish between Al and Si, since the actual difference in scattering is less than 4% for the two sites between model 1 & 2, and this would be an even smaller percentage of the overall neutron scattering.

As mentioned in Section 2, a very small amount of the J phase ($R_4Si_2O_7N_2$) (R = Y, Nd) exists as an impurity phase in the synthesized melilite samples, which is shown in the $Y_2Si_3O_3N_4$ and $Nd_2Si_{2.5}Al_{0.5}O_{3.5}N_{3.5}$ diffraction data shown in Figs 2 and 3 respectively as some weak unaccounted peaks in the patterns.

Chee *et al.* [15] have studied the atomic arrangement in Y–M′ with the composition ($Y_2Si_2AlO_4N_3$), using nuclear magnetic resonance techniques, and suggested that M′ is built up of AlO_4 and SiO_2N_2 structural units and that Al and O atoms form the tetrahedra situated at the origin and centre of the unit cell. It was found in the structure of $Y_2Si_3O_3N_4$ that the Si atoms at the origin and centre of the unit cell are surrounded by N atoms to form SiN_4 tetrahedra, which share corners with SiO_2N_2 to form a continuous sheet structure (see Fig. 4). For the structure of $Nd_2Si_{2.5}Al_{0.5}O_{3.5}N_{3.5}$, seven N atoms and one O atom are statistically distributed among the tetrahedra to form $SiN_{3.5}O_{0.5}$ in model 1 and $(Si_{0.5}Al_{0.5})N_{3.5}O_{0.5}$ in model 2. These tetrahedra are linked by two $(Si_{0.75}Al_{0.25})O_{2.25}N_{1.75}$ and $SiO_{2.25}N_{1.75}$ units in model 1 and 2 respectively. In order to confirm the positions of the N and O atoms in the $Nd_2Si_{2.5}Al_{0.5}O_{3.5}N_{3.5}$ structure, a refinement exchanging the positions of seven N atoms and seven O atoms and using model 2 for the distribution of Si and Al atoms was tried, which resulted in a rise of the R_F value from 0.078 to 0.112.

According to results obtained in previous work [4] both the *a* and *c* axes of the R–M′ unit cell increase continuously in length with increasing Al substitution. The *c*/*a* ratios of R–M′ in the same rare earth element samples were almost constant, however, which implies that the structural changes in R–M′ with the same rare earth element are isotropic. The results of the structural analyses of $Y_2Si_3O_3N_4$ and $Nd_2Si_{2.5}Al_{0.5}O_{3.5}N_{3.5}$ in the present work indicate that the distribution of the Si(Al), O, N atoms in the M/M′ phases do not change. Comparing the interatomic distances in $Y_2Si_3O_3N_4$ and $Nd_2Si_{2.5}Al_{0.5}O_{3.5}N_{3.5}$ listed in Table III, it is found that the average distance in the Nd-polyhedron of $Nd_2Si_{2.5}Al_{0.5}O_{3.5}N_{3.5}$ is distinctly longer than in the Y-polyhedron of $Y_2Si_3O_3N_4$, while the Si–N bond distance is shorter. Since the ionic radius of Al is larger than that of Si, it is likely that Al should be situated at the 4/e site of space group $P\bar{4}2_1m$ since the Si–N distance in (Si/Si, Al)1 $-$ $O_{2.25}N_{1.75}$ is longer than in $Y_2Si_3O_3N_4$, and the limit of substitution of Al for Si in R–M′ is due to the bond lengths in the tetrahedra in the R–M′ structures.

Acknowledgements

The authors are indebted to Profs. Mats Nygren and Thommy Ekström for their active interest and encouragement in this work. The National Natural Science Foundation, China, and the state Key Lab of High Performance Ceramics and Superfine Microstructure, Chinese Academy of Sciences are thanked for financial support.

References

1. S. SLASOR, K. LIDDEL and D. P. THOMPSON, *Br. Ceram. Proc.* **37** (1986) 51.
2. P.-O. KÄLL and T. EKSTRÖM, *J. Eur. Ceram. Soc.* **6** (1990) 119.
3. Y. B. CHENG, *J. Amer. Ceram. Soc.* **77** (1994) 143.
4. P. L. WANG, H. Y. TU, W. Y. SUN, T. S. YEN, M. NYGREN and T. EKSTRÖM, *J. Eur. Ceram. Soc.* **15** (1995) 689.
5. P. L. WANG, W. Y. SUN and T. S. YEN (D. S. YAN), *Mater. Res. Soc. Symp. Proc.*, Vol. 287, I.-W. Chen, P. F. Becher, M. Mitomo, G. Petzow, T. S. Yen (MRS Pittsburgh, Pennsylvania, 1993) p. 387.
6. J. PERSSON, T. EKSTRÖM, P. O. KÄLL and M. NYGREN, *J. Eur. Ceram. Soc.* **11** (1993) 363.
7. W. Y. SUN, D. S. YAN, L. CUO, H. MANDAL and D. P. THOMPOSON, *ibid.* **15** (1995) 349.
8. K. H. JACK, in "Non-Oxide Technical and Engineering Ceramics", edited by S. Hampshire (Elsevier Applied Science, London, 1986) p. 1.
9. K. S. CHEE, Y. B. CHENG, M. E. SMITH and T. J. BASTOW (private communication).
10. J. V. SMITH, *Amer. Mineral.* **38** (1953) 643.
11. H. M. RIETVELD, *J. Appl. Crystallogr.* **2** (1969) 65.
12. K. E. JOHANSSON, T. PALM and P.-E. WERNER, *J. Phys. E.: Sci. Instrum.* **13** (1980) 1289.
13. P.-E. WERNER, *Arkiv Kemi* **31** (1969) 513.
14. D.B. WILES, A. SAKTHIVEL and R. A. YOUNG, "User's Guide to Program DBW32s for Rietveld Analysis of X-ray and Neutron Powder Diffraction Pattern (Version 8804)", School of Physics, Georgia Institute of Technology, Atlanta, USA (1988).
15. K. S. CHEE, Y. B. CHENG and M. E. SMITH, *Chem. Mater.* **7** (1995) 982.

Received 17 March 1995
and accepted 18 March 1996